Relativistic band structure of Si, Ge, and GeSi: Inversion-asymmetry effects

U. Schmid, N. E. Christensen, and M. Cardona
Max-Planck-Institut für Festkörperforschung, Heisenbergstrasse 1, Postfach 80 06 65, D-7000 Stuttgart 80, Federal Republic of Germany
(Received 23 October 1989)

We present relativistic (including spin) linear muffin-tin orbitals (LMTO) calculations of the band structures of Si, Ge, and zinc-blende-like GeSi. The errors in excitation energies introduced by the use of the local-density approximation to the exchange-correlation potential are corrected with "*ad hoc*" potentials placed at the atomic sites. Effective masses, matrix elements of **p**, and Luttinger parameters are evaluated. Special emphasis is placed on the effects of inversion asymmetry in GeSi, such as ionicity and spin splittings. The former is very small, probably with Ge acting as the cation. The latter are appreciable and can be related to the asymmetry in the spin-orbit splittings of both constituent atoms. A detailed study of these spin splittings is made, also with the help of $\mathbf{k}\cdot\mathbf{p}$ perturbation theory. The coefficients of terms linear and cubic in k around $\mathbf{k}=\mathbf{0}$ are obtained. They should be experimentally observable when high-quality samples become available and should help to understand similar splittings in $(Ge)_n/(Si)_m$ (n,m odd) superlattices.

I. INTRODUCTION

Recent advances in the growth of ultrathin $(Ge)_n/(Si)_m$ superlattices[1-4] using molecular-beam epitaxy (MBE) have made possible the growth of layered, alternating planar heterostructures, down to one atomic monolayer of Si and Ge. The resulting $(Ge)_1/(Si)_1$ superlattice ("GeSi") has the zinc-blende structure [space group T_d^2 ($F\bar{4}3m$)], and thus lacks a center of inversion. The inversion asymmetry is reflected in the large difference in spin-orbit splitting, which for the p valence electrons amounts to $\Delta_0 \approx 300$ meV in Ge but only about 44 meV in Si.

Inversion symmetry is preserved when there is an even number of monolayers of either material in the superlattice.[5,6] Time reversal plus inversion symmetry require at a general **k** point that all states be at least doubly degenerate. Nonrelativistic band-structure calculations on $(Ge)_n/(Si)_n$ superlattices have focused primarily on such structures.[6-12] For $(Ge)_n/(Si)_m$ superlattices with both n and m odd[5] [space groups T_d^2, D_{2d}^5 ($P\bar{4}m2$), and D_{2d}^9 ($I\bar{4}m2$)], however, there is no inversion symmetry, and depending on the direction of **k** and the double-group symmetry of the states, only some states remain doubly degenerate. For the $m=n=1$ zinc-blende structure, which we want to investigate in this paper, only along $\langle 100\rangle$ (Δ direction) do all the states remain doubly degenerate, whereas along $\langle 111\rangle$ states of $\Lambda_{4,5}$ symmetry split, while those of Λ_6 do not.[13,14] For other points in the Brillouin zone all states split by spin-orbit interaction. The splittings are expected to be largest along the $\langle 110\rangle$ directions, and have previously been calculated for a variety of other zinc-blende-type semiconductors.[15-18]

The GeSi system can be regarded as a prototype for all noninversion $(Ge)_n/(Si)_m$ superlattices as its cubic structure is unaffected by the internal strain built into $(Ge)_n/(Si)_m$ superlattices which results, of course, from the large lattice mismatch of about 4%. This means that the band structure is not complicated by effects due to biaxial strains at the different layers under various conditions of pseudomorphic growth, and that relativistic spin splittings can easily be interpreted. Thus, the GeSi system is of principal interest as a basis for the understanding of Ge/Si superlattices, which have attracted much experimental and theoretical attention because of the possibility of obtaining a direct or quasidirect semiconductor material based on Si.[1-8,10-12] Such a superlattice could be a component of an integrated optoelectronic device, based on well-established silicon technology. In this case the transport properties of GeSi should be important. They are, however, affected by the spin splittings around the band extrema. These splittings are extremely small, even smaller than for most of the III-V compounds, where they can amount to as much as a few tenths of an eV.[18] In some II-VI compounds, however, they can reach values up to 0.8 eV.[19] When expanded around $k=0$ these splittings are of third order in k (the distance in **k** space to the extrema), although for some particular extrema (e.g., the top of the valence bands) a linear term appears. These splittings can be verified and measured with optical-pumping experiments, which measure the spin-relaxation time by means of the Hanle effect,[20,21] or other forms of polarized luminescence,[22] spin-polarized photoemission,[23] and magneto-optical experiments,[24] but certainly the quality of the existing samples has to be improved before these effects actually show up in Ge/Si superlattices. The coefficient γ of the k^3 terms, including its sign, can be obtained from the strengths of the electric-field-induced spin-resonance signals.[25,26]

In this paper we present detailed *ab initio* calculations of the relativistic band structure of Si, Ge, and GeSi performed with the linear muffin-tin orbitals (LMTO) method.[27,28] They are used in Sec. III to evaluate the effective mass of the Γ_1 ($\Gamma_{2'}$) conduction band, m_c, and

the Luttinger parameters $\gamma_1,\gamma_2,\gamma_3$, which describe the warping of the valence band at the Γ point.[29–32] In addition, detailed calculations of the matrix element P' are described. In Sec. IV we calculate the spin-orbit-coupling parameter Δ^- (between the Γ_{15} conduction and valence bands) for GeSi with the LMTO method, and give a tight-binding estimate for Δ^-. The cubic and linear terms of the inversion-asymmetry spin splittings calculated along different lines of $\mathbf{k}$ space are presented in Sec. V, together with estimates from the $\mathbf{k}\cdot\mathbf{p}$ method.[14,15,30–33] In Sec. VI we present calculations of the ionicity and transverse effective charge in GeSi. Finally, Sec. VII contains a summary of the results.

II. LMTO BAND-STRUCTURE CALCULATIONS

The electronic band structure of Si, Ge, and GeSi are calculated here within the framework of local-density-functional theory[34] by means of the self-consistent, relativistic LMTO method.[27] We include "empty spheres,"[28] that is, atomic spheres with no net nuclear charge, in the empty tetrahedral sites in order to obtain a close-packed structure and the so-called "combined-correction term."[35]

We include s, p, and d partial waves for the wave functions in each atomic sphere, and also for the empty spheres. Spin-orbit interaction is treated in all calculations as a perturbation to the scalar-relativistic Hamiltonian. The splittings which we want to examine for the GeSi compound are due to spin-orbit interaction, as well as the ordinary spin-orbit splittings which occur at high-symmetry points at the Brillouin zone of Si and Ge (Δ_0, Δ_0', and Δ_1). For this reason we have included spin-orbit interaction in all the calculations as a perturbation to the scalar-relativistic Hamiltonian. This requires a Hamiltonian matrix of dimension 72×72, with four "atoms" in the basis. Furthermore, the comparison of calculated with experimental values in the case of Si and Ge gives us a good feeling of how accurate our GeSi results actually can be.

The Si atom has no d states, and the $3d$ levels of Ge lie so deep that it suffices to treat them as "frozen"-renormalized-core-like states. As indicated in the Introduction, the structure of Si, Ge, and GeSi, respectively, is the simple-cubic one. We take for a_0 (the cubic lattice constant) of GeSi the average of the bulk values of Si ($a_0=5.43$ Å) and Ge ($a_0=5.66$ Å). The strain is fully accommodated by the tetrahedral bonds of the cubic structure.

In order to obtain a consistent definition of the sign of Δ^- and of the matrix elements P, P', Q, and P''' of $\mathbf{p}$, which we define as

$$P=i\langle\Gamma^v_{15,x}|p_x|\Gamma_1\rangle,\quad P'=i\langle\Gamma^c_{15,x}|p_x|\Gamma_1\rangle\ ,$$
$$Q=i\langle\Gamma^v_{15,x}|p_x|\Gamma^c_{15,x}\rangle,\quad P'''=i\langle\Gamma^v_{15,x}|p_x|\Gamma'_1\rangle\ , \tag{2.1}$$

it is crucial to clearly specify the positions chosen for the two constituent atoms, and the phase of the wave functions.[17,18] We choose them to be real, as depicted in Fig. 1. Note that the Si atom has been chosen to be at the origin, while the Ge is at $(a_0/4)(1,1,1)$. This convention is consistent with the one which was earlier used,[18] if we call the Si atom an "anion." The justification for this choice will be given in Sec. III B in terms of tight-binding estimates, and in Sec. VI. Nonetheless, we point out that the ionicity of the Si—Ge bond is very weak.[9] Thus the role of the Ge as a cation cannot be considered as firmly established in the absence of experimental verification. This choice results in a positive sign of P and Q, which can easily be verified from Fig. 1 by replacing p_x by $-i\partial/\partial x$. We can also see from this figure that the terms which contribute to P' almost cancel, so that P' is very small. The sign of P' is a delicate question and will be discussed in Sec. III A.

The crystal potentials are obtained by iterating the one-electron wave equation to self-consistency with an effective potential where exchange and correlation are treated in the local-density approximation (LDA) of the form constructed by Ceperley and Alder[36] as parametrized by Perdew and Zunger.[37] Such straight LDA calculations are known to yield correct ground-state properties, but band gaps that are much smaller than the experimental excitation energies.[35] An "*ad hoc*" correction can be made by adding external potentials $V_a(\mathbf{r})$ of the form[38]

$$V_a(\mathbf{r})=V_0\frac{r_0}{r}\exp[-(r/r_0)^2]\ , \tag{2.2}$$

centered at each atomic site a. These sharply peaked, δ-like potentials are added at the real-atom sites as well as at those of the empty spheres, for which there is only one type in the elemental semiconductors Si and Ge. The values of the potential parameters V_0 and r_0 are chosen

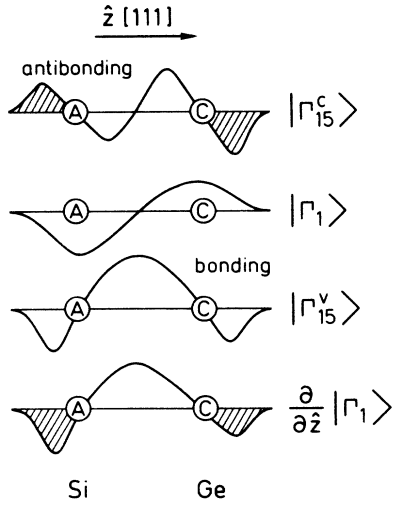

FIG. 1. Schematic diagram which demonstrates the phase convention of the Γ^c_{15}, Γ_1, and Γ^v_{15} wave functions. The Si atom is taken to be at the origin, and thus is identical with the anion (A), whereas the Ge atom can be regarded as the cation (C). For the p-like eigenstates $\Gamma^{c,v}_{15}$, the component along $\mathbf{k}$ along the [111] direction is shown. Note that the sketch of Γ^v_{15} in Fig. 1 of Ref. 18 is in error.

TABLE 1. Parameters V_0 (in units of hartree) and r_0 (in units of bohr) of the potentials [see Eq. (2.2)] added at the different sites to correct for the band gaps.

	Atomic site		Empty sphere	
	V_0	r_0	V_0	r_0
Si	268.187	0.015	7.583	0.55
Ge	180.0	0.015	4.0	0.7

such that the gaps at the three different symmetry points, Γ, X, and L, agree with experimental values at low temperatures; these values are listed in Table I. The correction potentials determined for Si and Ge are transferred to the self-consistent calculations for the GeSi compound. As this is an obvious choice for the real-atom sites, inevitable due to the lack of experimental values of the band gaps, this is not so for the two different empty spheres which occur in the compound. We choose for the "$E2$" site, which is the one that is surrounded by Si atoms, the parameter derived for the empty sphere in the bulk Si calculations, and for the "$E1$" sites the Ge values, as shown in Table I. To obtain an estimate of the error which could be introduced by this choice, we exchanged the parameters of the two types of empty spheres, an extreme and physically unreasonable choice which leads to "Si" empty spheres, surrounded by Ge-atom sites, and vice versa. The changes of the band structure were minimal; the biggest difference occurred at X_6^c and amounted to 0.14 eV. Apparently, the adjusting potential parameters of the two empty spheres are too close to have a decisive influence on the band structure.

The change of the band structure produced by the introduction of the extra δ-like potentials when iterated self-consistently is rather intricate. Whereas they strongly push up all of the s-like conduction bands, as desired, they only slightly affect the valence states, and the p-like conduction states, which are still calculated to lie somewhat lower than experimentally determined. That means

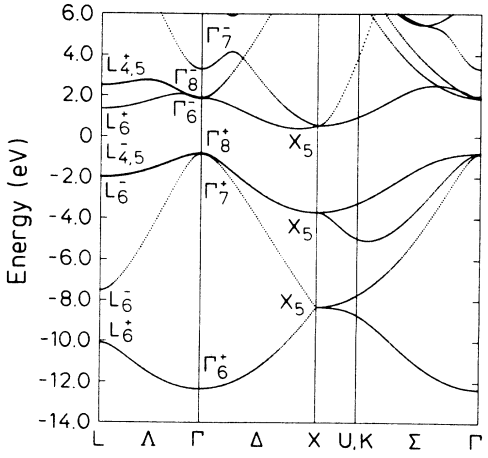

FIG. 2. Relativistic energy-band structure of Si along high-symmetry lines, as calculated in the LDA, but with the adjusting potentials included self-consistently.

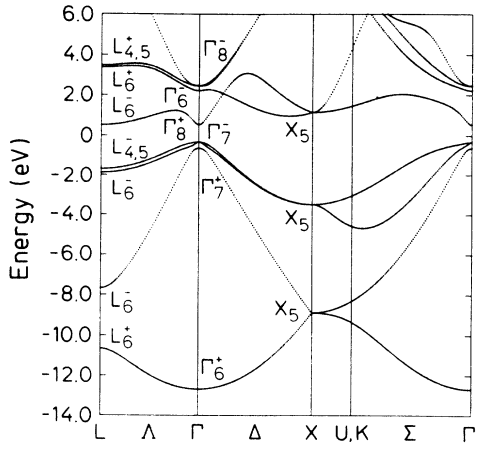

FIG. 3. Relativistic energy-band structure of Ge along high-symmetry lines as calculated in the LDA, but with the adjusting potentials included self-consistently.

that the results for the E_0 gap are usually very good, while the E_0' gap is underestimated. The incorrect position of the low-lying p-like conduction band affects, in turn, the warping of the Γ_8^v valence band, and leads to incorrect Luttinger parameters. In Sec. III we will give a detailed recipe of how to cure this problem within the framework of the $\mathbf{k}\cdot\mathbf{p}$ method.

The LMTO band structures of Si, Ge, and GeSi are calculated as described and shown in Figs. 2–4. Since the diamond structure does have inversion symmetry, all bands of Si and Ge are twofold degenerate, whereas only few bands of the GeSi compound along particular symmetry lines ([111] and [100]) maintain this degeneracy. As expected, the splittings along the Σ ([110]) line are the

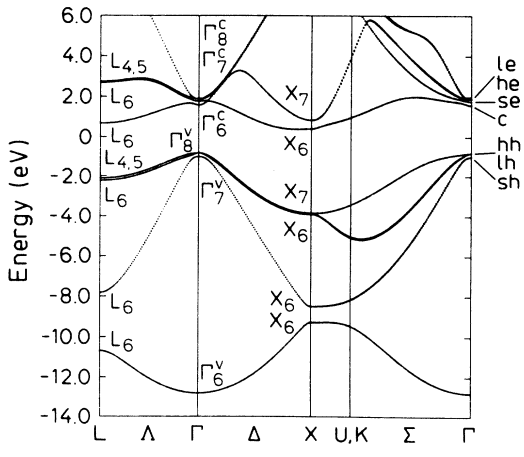

FIG. 4. Relativistic energy-band structure of the zinc-blende-type compound GeSi along high-symmetry lines as calculated in the LDA, but with the adjusting potentials included self-consistently. The labels sh (split-off hole), lh (light hole), hh (heavy hole), c (Γ_6^c), le (light electron), and he (heavy electron) band, refer to the notation used in Sec. V.

TABLE II. Calculated and experimental gap energies and spin-orbit splittings at points of high symmetry. All energies are in eV.

	Si		Ge		GeSi
	LMTO	Expt.	LMTO	Expt.	LMTO
E_0	4.135	4.185	0.854	0.887	2.407
Δ_0	0.050	0.044	0.305	0.296	0.186
E_0'	2.671	3.40	2.537	3.01	2.599
Δ_0'	0.039	0.03–0.04[a]	0.237	0.200	0.118
Δ^-	0		0		0.130
E_1	3.326	3.45	2.194	2.222	2.776
Δ_1	0.032	0.03[a]	0.190	0.19	0.114
E_2	4.243	4.44	4.636	4.49	4.238
Δ_2	0		0		0.072

[a]Calculated, see Ref. 32.

largest, although not possible to discern in Fig. 4. To get a good picture of the splittings, the reader is directed to Figs. 6–8 in Sec. V, where the pure splittings along the [110] and [111] directions are depicted.

Table II shows the main energy gaps and the spin-orbit splittings of the three materials at the three points of high symmetry, Γ, L, and X. Except for the problem with E_0' described above, all values for Si and Ge are in excellent agreement with the experiments. The spin-orbit splitting of X, Δ_2, is also due to the lack of inversion symmetry in the zinc-blende structure and does not occur in diamond-type materials. The same holds for the gap between the X_6-X_6 lowest valence states, which was calculated to be 0.786 eV in GeSi.

The calculated band structures of GeSi have an indirect gap. The conduction-band valley is located at about $0.87k_0$ along the Δ direction, k_0 being the zone-edge lattice vector along [100]. We found the energy gap to be 1.22 eV. This is only slightly larger than what we calculated for Si (1.18 eV) at $0.83k_0$, which compares very well with experimental data;[32] the splitting of the X_1 states of the diamond structure into X_1-X_3 is responsible for the increase in k_0.

Overlooking these splittings, the rough features of the band structure along Δ are very similar to those of Si, except for the region close to Γ. Surprisingly, this holds for the Λ direction too. The electronic properties of GeSi should therefore be much like those of Si.

III. EFFECTIVE MASSES, LUTTINGER PARAMETERS, AND MATRIX ELEMENTS

A. LMTO calculations

In order to study the finer structure around $\mathbf{k}=\mathbf{0}$, we divide the Brillouin-zone symmetry lines along the [100], [110], and [111] directions into a dense $\mathbf{k}$ mesh with up to 1500 points. By fitting a straight line to the calculated electronic energies versus k^2 in the immediate vicinity of point Γ, the slopes yield effective masses for the different directions.

The effective masses of the s-like conduction bands $\Gamma_{2'}$ (Γ_1), m_c, and of the spin-split Γ_7 valence bands, m_{so}, are isotropic, in contrast to the heavy- and light-hole masses, which show strong warping described by the Luttinger parameters γ_1, γ_2, and γ_3. A simple calculation yields for the effective masses (in units of the free-electron mass) at point Γ along the Δ direction,

$$\frac{1}{m_{001}^{\mathrm{hh,lh}}}=\gamma_1\pm 2\gamma_2 , \tag{3.1a}$$

and along the Λ direction,

$$\frac{1}{m_{111}^{\mathrm{hh,lh}}}=\gamma_1\pm 2\gamma_3 , \tag{3.1b}$$

The values for the Luttinger parameters we calculated by fitting the corresponding LMTO masses are presented in Table III, together with the effective masses m_c and m_{so}.

Whereas m_c and m_{so} agree reasonably with experimental values, this is not so for the Luttinger parameters. When one expresses them within the framework of the $\mathbf{k}\cdot\mathbf{p}$ theory in terms of the matrix elements of $\mathbf{p}$,[18,30,31] it becomes clear why that is so: they contain the matrix element M, which is inversely proportional to $E_0'+2\Delta_0'/3$. As E_0' is basically the only gap which is reproduced incorrectly by our LMTO calculations, we decided to calculate M, and rescale it with the experimental values for E_0', and thus obtained "experimentally corrected" Luttinger parameters. These values are also shown in Table III and agree well with the experimental data. For the "experimental" value E_0' of GeSi we took the average of the values of Si and Ge, 3.2 eV. This is also in agreement with results obtained using Van Vechten's interpolation formula.[39]

The matrix elements Q were calculated from[18]

$$2Q^2=(\gamma_1-2\gamma_2+1)(E_0'+\tfrac{2}{3}\Delta_0') . \tag{3.2}$$

Again, uncorrected LDA values, and values which are corrected by using the measured E_0', are presented in Table III and compared to experimental data. The "adjusted" matrix elements are generally about 10% lower than the values calculated from experimental data. This is consistent with earlier discrepancies following from parametrized $\mathbf{k}\cdot\mathbf{p}$ calculations[18] and can be attributed to the approximations which are introduced in the LMTO calculations, namely the spherical charge symmetrization

TABLE III. Effective masses of the lowest conduction bands (m_c), and the split-off bands (m_{so}), in a.u. The Luttinger parameters labeled with footnote a were calculated from Eqs. (3.1); those labeled with footnote b have been adjusted for the experimental E_0', as described in Sec. III. The p matrix elements P and Q were either calculated from Eqs. (3.2) and (3.3) (footnote a) or were adjusted with experimental values (footnote b).

	Si		Ge		GeSi
	LMTO	Expt.	LMTO	Expt.	LMTO
m_c	0.209		0.048	0.037	0.129
m_{so}	0.244	0.234	0.119	0.095	0.192
γ_1[a]	4.14		11.1		5.61
γ_1[b]	3.74	4.29	10.7	13.4	5.21
γ_2[a]	0.20		3.20		0.75
γ_2[b]	0.40	0.34	3.40	4.24	0.94
γ_3[a]	1.31		4.65		2.38
γ_3[b]	1.41	1.45	4.75	5.69	2.48
Q[a]	0.486		0.539		0.505
Q[b]	0.499	0.540[c]	0.541	0.607[c]	0.498
P	0.537	0.695[d]	0.557	0.655[d]	0.547
$\lvert P'\rvert$					<0.03

[a]LDA calculation with δ-like potentials.
[b]Adjusted for experimental E_0'.
[c]Calculated from experimental Luttinger parameters, and experimental E_0', Δ_0'. Experimental values are from Ref. 32 (see Table II).
[d]Calculated from experimental E_0 and m_c.

and the incomplete conduction-band adjustments. The matrix elements P' as defined in Eq. (2.1) only occurs in zinc-blende-type materials and is zero by symmetry in the diamond structure. It can be estimated with[30,31,40]

$$\frac{1}{m_c}=1+2P^2\left[\frac{1}{3}\left[\frac{2}{E_0}+\frac{1}{E_0+\Delta_0}\right]-\left[\frac{P'}{P}\right]^2\frac{1}{E_0'-E_0}\right] . \tag{3.3}$$

The value of P for GeSi is taken to be the average of the Si and Ge values, which can also be calculated using Eq. (3.3) by setting $P'=0$.

Within the accuracy that we can determine m_c, the calculation yields $|P'|\leq 0.03$. This means $|P'|\leq 0.05P$, an unusually small value for zinc-blende-type materials, which reflects the strong similarity of the corresponding wave functions of Si and Ge. For III-V compounds, P' amounts to about $0.35P$.[18]

B. Tight-binding estimate of P'

P' can also be estimated with a simple tight-binding argument. Assuming that the Γ_{15}^v and Γ_{15}^c wave functions are obtained as bonding and antibonding linear combinations of the Si, $|\mathrm{Si}\rangle$, and Ge, $|\mathrm{Ge}\rangle$, p states, we can write

$$\begin{aligned}|\Gamma_{15}^v\rangle&=\alpha|\mathrm{Si}\rangle+\beta|\mathrm{Ge}\rangle ,\\ |\Gamma_{15}^c\rangle&=\beta|\mathrm{Si}\rangle-\alpha|\mathrm{Ge}\rangle .\end{aligned} \tag{3.4}$$

If we assume the same for the s states, which we distinguish from the p states with a prime,

$$|\Gamma_1\rangle=\beta'|\mathrm{Si}'\rangle-\alpha'|\mathrm{Ge}'\rangle , \tag{3.5}$$

we can calculate P' via Eq. (2.1). Defining the matrix elements

$$P'_{\mathrm{inter}}=i\langle \mathrm{Ge}|p_x|\mathrm{Si}'\rangle\approx i\langle \mathrm{Si}|p_x|\mathrm{Ge}'\rangle$$

and

$$P'_{\mathrm{intra}}=i\langle \mathrm{Ge}|p_x|\mathrm{Ge}'\rangle\approx i\langle \mathrm{Si}|p_x|\mathrm{Si}'\rangle ,$$

we get two limiting cases:

$$\text{(i)}\quad P'_{\mathrm{inter}}=0:\quad P'\approx P'_{\mathrm{intra}}=\frac{\alpha\alpha'+\beta\beta'}{\alpha\beta'-\alpha'\beta} , \tag{3.6a}$$

$$\text{(ii)}\quad P'_{\mathrm{intra}}=0:\quad P'\approx P'_{\mathrm{inter}}=\frac{-\alpha\beta'-\alpha'\beta}{-\alpha\alpha'+\beta\beta'} . \tag{3.6b}$$

Referring to Eq. (3.4) and Fig. 1, we want to point out that $|\mathrm{Si}\rangle$ and $|\mathrm{Ge}\rangle$ are chosen to have the positive lobe to right, so that the coefficients $\alpha>0$ and $\beta<0$. They can be obtained from[41,42]

$$\eta=\frac{\alpha}{\beta}=\frac{-2H_{xx}}{E_p^{\mathrm{Si}}-E_p^{\mathrm{Ge}}+[(E_p^{\mathrm{Si}}-E_p^{\mathrm{Ge}})^2+4H_{xx}^2]^{1/2}} . \tag{3.7}$$

Here, E_p^{Ge} and E_p^{Si} are atomic term values that appear on the diagonal of the tight-binding Hamiltonian. H_{xx}, the composite overlap matrix element, is a function of the bond length d, and can be written for the zinc-blende structure as[42]

$$H_{xx}=1.28d^{-2} . \tag{3.8}$$

We calculated η from Eq. (3.7) to be -1.08 for GeSi. This follows from the fact that the term value of the "cation" (Ge) lies slightly above that of the "anion" (Si), which is also typical for other zinc-blende-type semiconductors and results in an antibonding wave function Γ_{15}^c, which is more cationlike, as depicted in Fig. 1. The ratio of the two coefficients α' and β' (both positive) of the s states, $\eta'=\alpha'/\beta'$, follows from an expression which is

equivalent to Eq. (3.7) and amounts to $\eta'=0.97$. This time, however, the s-state term value of Ge is lower in energy, compared to Si, so that the Γ_1 wave function is more concentrated on the Si side ("anionlike"), a situation which is not observed in III-V compounds and seems to be unique to GeSi. The consequences of this fact can easily be studied in Fig. 1. There, we see that terms contributing to P'_{intra}, i.e., terms which are determined by the "tails" of the functions $|\Gamma^c_{15}\rangle$ and $\partial/\partial\hat{z}|\Gamma_1\rangle$ (contributions from the hatched areas in Fig. 1), almost cancel, which means that P' is determined by P'_{inter}, i.e., the central part of those functions (between the A and C sites). Equation (3.6b) yields $P'\approx 0.05P\approx 0.03$. This is in excellent agreement with our previous result and also gives us the sign. Further support for a positive sign of P' is based on atomic term values from Ref. 43, which lead to $\eta=-1.16$ and $\eta'=0.92$. Note that this sign is only found from the tight-binding parameters obtained self-consistently for GeSi. If the separate parameters of Ge and Si are used, the opposite sign is found for P'.

We have also performed an empirical pseudopotential calculation of P' based on the parameters of Cohen and Bergstresser[44] for Ge and Si, and found $P'=-0.07$. The small magnitude of this P' is compatible with the other estimates, but the sign is the opposite of what we believe to be correct. This emphasizes the need for self-consistent calculations in order to obtain the correct sign of this small parameter.

IV. ESTIMATES OF Δ^- IN GeSi

A. LMTO estimates

We define the spin-orbit-coupling parameter Δ^- as[18]

$$\Delta^-=3\langle(\tfrac{3}{2}\tfrac{3}{2})_v|H_{\text{s.o.}}|(\tfrac{3}{2}\tfrac{3}{2})_c\rangle\ , \tag{4.1}$$

where $(\frac{3}{2}\frac{3}{2})_v$ represents the eigenvector of the Γ^v_{15} eigenstates. Taking the phase convention of Fig. 1 (both eigenstates are chosen real), Δ^- is real.

The magnitude of Δ^- can be determined by performing calculations for the Γ^v_{15} and Γ^c_{15} states both with and without the inclusion of spin-orbit interaction. Δ^- accounts for the fact that the ratio of upshift of the Γ_8 states to the downshift of the Γ_7 states is not 1:2, the scalar-relativistic value, but deviates slightly from it. This is illustrated in Fig. 5. Second-order perturbation theory yields, for these shifts,

$$\begin{aligned}\delta(\tfrac{3}{2})&=\frac{\Delta_0}{3}-\left[\left[\frac{\Delta^-}{3}\right]^2\Big/E'_0\right],\\ \delta(\tfrac{1}{2})&=-\frac{2\Delta_0}{3}-\left[\left[\frac{2\Delta^-}{3}\right]^2\Big/E'_0\right].\end{aligned} \tag{4.2}$$

Using this equation with the values $\delta(\frac{3}{2})=61.2$ meV and $\delta(\frac{1}{2})=-126.7$ meV, the calculation yields the values of Δ_0 and $|\Delta^-|$ as listed in Table II. Δ_0 is only 0.02 meV smaller than the splitting $\delta(\frac{3}{2})-\delta(\frac{1}{2})$.

B. Tight-binding estimate

Again, the minimum-basis tight-binding method[45] proves to be a useful tool, especially for the determination of the sign of Δ^-. From the spin-orbit Hamiltonian and under the approximation $|\alpha|=|\beta|$, which has been justified in the preceding section, we find

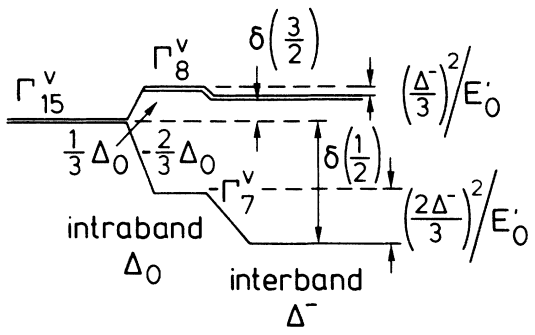

FIG. 5. Schematic diagram of the influence of Δ^- on the spin-orbit splitting of the Γ^v_{15} bands. Pure intraband terms yield the relativistic 1:3 ratio, which is not maintained when the interactions with the Γ^c_{15} band is included in second-order perturbation theory.

$$\Delta^-=\tfrac{1}{2}[\Delta_0(\text{Ge})-\Delta_0(\text{Si})]=128\ \text{meV}\ , \tag{4.3a}$$

$$\Delta_0=\Delta'_0=\tfrac{1}{2}[\Delta_0(\text{Ge})+\Delta_0(\text{Si})]=175\ \text{meV}\ , \tag{4.3b}$$

which, except for Δ'_0, hardly deviates from LMTO values listed in Table II for GeSi. The stronger deviation of Δ'_0 can be attributed to a higher mixing of d states in Γ^c_{15}, compared to Γ^v_{15}, which has been ignored in our tight-binding considerations.

V. INVERSION-ASYMMETRY SPIN SPLITTING IN GeSi

A. Cubic terms along the [110] direction

Along the Σ direction all bands split in zinc-blende-type materials. The splitting in energy can be written for small k as[13,14]

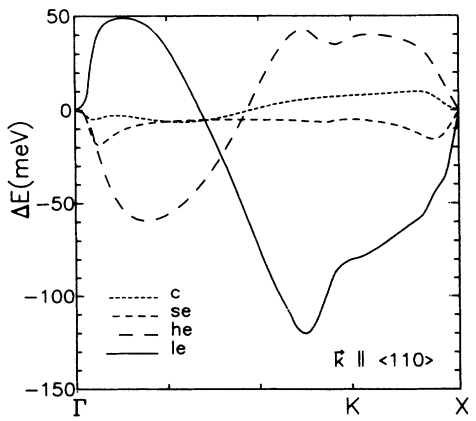

FIG. 6. Spin splittings of the lowest conduction bands in GeSi for **k** along the [110] direction as calculated with the LMTO method.

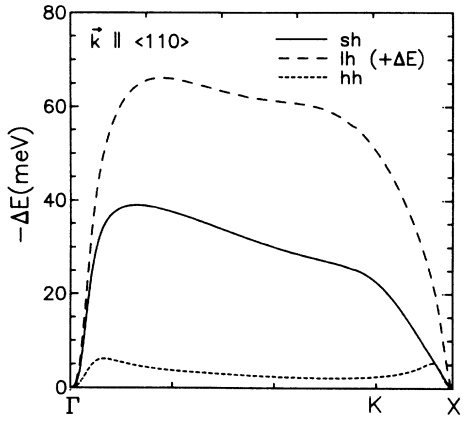

FIG. 7. Spin splittings of the highest valence bands in GeSi for **k** along the [110] direction as calculated with the LMTO method.

$$\Delta E = \gamma k^3 , \tag{5.1}$$

where we define the sign to be positive if the Σ_4 state is above the Σ_3 state.[18] To denote the splittings of the Γ_6 conduction band, and the Γ_8^v, Γ_7^v and Γ_8^c, Γ_7^c bands, we shall use γ with the subscripts c, sh, hh, lh, se, le, and he, as indicated in Fig. 4. These symbols will also appear on the following figures. In Figs. 6 and 7 we present the splittings for the conduction and valence bands, respectively, as a function of **k** along [110]. Figures 9 and 10 show the splitting near Γ with expanded energy and **k** scales.

We have calculated the different γ's from our LMTO data by fitting the energy difference ΔE of the split-up bands to k^3, the k values being within a very dense k mesh close to Γ. When required by symmetry, we added a linear parameter to the fit. We will discuss the linear term in the next subsection in detail.

The calculated γ's are given in Table IV. There, they are also compared to values which we calculated using expressions derived from third order (in $\mathbf{k}\cdot\mathbf{p}$) perturbation theory from states which include exactly Δ_0, Δ_0', and Δ^-. In contrast to an approach that has been used earlier,[18] namely the evaluation of the necessary parameters by the diagonalization of the 16×16 $\mathbf{k}\cdot\mathbf{p}$ Hamiltonian, we will use our LMTO values with and without experimental adjustment of E_0' as described in Sec. III. These calculations have the advantage of giving the sign for γ which cannot be determined from our LMTO eigenvalues. We have, however, checked the sign carefully with LMTO calculations, by adding to the Hamiltonian in the $\mathbf{k}\|[110]$ calculations a magnetic field parallel to the $[1\bar{1}0]$ direction, acting on the spin. From symmetry considerations we found that for both the $(\frac{1}{2},\pm\frac{1}{2})$ and $(\frac{3}{2},\pm\frac{1}{2})$ states the Σ_3 states have a prevailing projection of the $|\downarrow\rangle$ spin along the $[1\bar{1}0]$ direction. States with spin parallel to the magnetic field decrease in energy, while antiparallel states increase.

1. Γ_1 band along the [110] direction

According to fourth-order $\mathbf{k}\cdot\mathbf{p}$ perturbation theory, γ_c is given by Eq. (5.7) of Ref. 18. We point out that not all terms which contain the matrix element P' can be neglected, although P' is very small. This is especially true for the second term ($\mathcal{B}$), as it also contains $(E_0-E_0')^2$, a rather small value, in the denominator. Similar problems also occur in the calculation of other γ's, with the following two consequences: (1) the γ_c's are very sensitive to the choice of the value for P', which is not known very accurately, and (2) the convergence of fourth-order perturbation theory due to the proximity of E_0 and E_0' is not always guaranteed (in particularly, when matrix elements proportional to $\Delta_0'\approx E_0-E_0'$ are included). We found, however, that the value $P'\approx+0.015$, slightly reduced from the value estimated in Sec. III, gives reasonable results for all γ's.

Using the LMTO parameters of Table III, we calculated the various components of γ_c to be

$$\gamma_c = 0.6\ (=\mathcal{A}) + 4.9\ (=\mathcal{B}) - 12.4\ (=\mathcal{C}) - 0.2\ (=\mathcal{D})$$
$$= -7.1 \text{ a.u.} , \tag{5.2}$$

which is sufficiently close to our LMTO value (-9.7 a.u.).

2. Γ_{15}^v band along the [110] direction

In this case, the second-order $\mathbf{k}\cdot\mathbf{p}$ interaction with Γ_1 via the matrix element P gives the main contribution to the Luttinger parameters, i.e., to the band curvatures; since this interaction is isotropic $[(\gamma_2-\gamma_3)/\gamma_1 \ll 1]$, the [110] wave functions still have the form of angular-momentum functions $|j,m_j\rangle=(\frac{3}{2},\pm\frac{3}{2}),(\frac{3}{2},\pm\frac{1}{2})$ with the quantization axis along the [110] direction. Fourth-order

TABLE IV. Values of the coefficient of the spin splittings Γ_1, Γ_{15}^v, and Γ_{15}^c bands proportional to k^3 (γ's, in hartree bohr^3) and k (C_k, C_k', in hartree bohr) as obtained from a fit of the data which are shown in Figs. 8–10. The pure LMTO values are compared to those obtained from the $\mathbf{k}\cdot\mathbf{p}$ perturbation theory (PT) and experimentally adjusted (expt. adj.) values, as described in Sec. V.

	γ_c	γ_{lh}	γ_{sh}	γ_{se}	γ_{le}	γ_{he}	C_k	C_k'
LMTO	−9.7	19.6	−13.5	−9.8	23.8	−6.5	−1.85	−3.07
$\mathbf{k}\cdot\mathbf{p}$ (PT)	−7.1	22.1	−20.4	−9.6	7.1			
$\mathbf{k}\cdot\mathbf{p}$ (expt. adj.)	−5.5	28.5	−26.4	−4.5	4.7			

$\mathbf{k}\cdot\mathbf{p}$ perturbation theory predicts $\gamma_{\rm hh}$ (the k^3 coefficient for the heavy hole) to be zero. This does not mean that there is no splitting, as there are also orders higher than k^3, such as k^5. The coefficient for the light-hole band is given by [note that Eq. (5.9) of Ref. 18 contains an error in the sign]

$$\gamma_{\rm lh}=-\frac{4PP'Q}{3E_0\bar{E}'_0}+\frac{4P^2Q\Delta^-}{3E_0\bar{E}'_0\Delta_0}+\frac{2Q^3\Delta^-}{3E'^2_0\Delta_0}$$
$$=(-0.6+16.2+6.5)\text{ a.u.}=22.1\text{ a.u.} \quad (5.3)$$

Again, this compares very well with our LMTO value (19.6 a.u.). The γ coefficient of the split-off band, $\gamma_{\rm sh}$ can be obtained from Eq. (5.3) by adding the corresponding spin-orbit splittings Δ_0 and Δ'_0 to E_0 and E'_0, respectively, and reversing the sign (for values, see Table IV).

3. Γ^c_{7s} along the [110] direction

The Γ^c_7 are given by $(\frac{1}{2},\pm\frac{1}{2})$-like combinations of orbital and spin wave functions, with [110] being the quantization axis. Neglecting terms in P'^2 and taking for P''' the Ge value,[46] 0.57 a.u., and for $E'''_0=8.4$ eV, this leads to [see Eq. (5.10) of Ref. 18]

$$\gamma_{\rm se}=-\frac{4PP'Q}{3(E'_0-E_0)(E'_0+2\Delta_0/3)}$$
$$+\frac{2Q^3\Delta^-}{3(E'_0+2\Delta_0/3)^2\Delta'_0}$$
$$-\frac{4(P''')^2Q\Delta^-}{3(E'''_0-E'_0)(E'_0+2\Delta_0/3)\Delta'_0}$$
$$=(-7.8+9.4-11.2)\text{ a.u.}=-9.6\text{ a.u.} \quad (5.4)$$

Here, the fourth term is due to the interaction with the Γ'_1 band (the next-higher Γ_1 conduction band).

If the Γ^c_8 wave functions for $\mathbf{k}$ along the [110] direction corresponded, to a good approximation, to angular-momentum states, $\gamma_{\rm le}$ would be obtained from Eq. (5.4) by adding Δ'_0 to E'_0, and reversing all signs.

Whereas the agreement with the LMTO calculations is excellent for $\gamma_{\rm se}$, taking the problems discussed earlier into account, the $\gamma_{\rm le}$ value differs by more than a factor 3 (see Table IV). We conclude that there is a strong mixing of the $|\frac{3}{2},\pm\frac{3}{2}\rangle$ and $|\frac{3}{2},\pm\frac{1}{2}\rangle$, which affects $\gamma_{\rm le}$ and introduces a finite cubic term coefficient $\gamma_{\rm he}=-6.5$ a.u. in the heavy-electron bands (Table IV). Some additional interactions may also be necessary to explain the large LMTO value of $\gamma_{\rm le}$.

4. Discussion

Except for the cases discussed earlier, we obtain, in general, good agreement between the values derived from our LMTO calculations and those calculated from $\mathbf{k}\cdot\mathbf{p}$ perturbation theory, i.e., the first and second rows of Table IV. This means that both calculations are consistent and lends further support to our estimates of Δ^- and P'. The parameters obtained from LMTO calculations can be regarded as *ab initio*, as they include all states of s, p, and d symmetry, particularly the core levels. Nevertheless, this method has some deficiencies: the gap adjustments and the spherical charge symmetrization in each of the spheres. We pointed out already that especially the last point is the probable reason why the calculated matrix elements of $\mathbf{p}$ are too small. The gap adjustment, on the other hand, is not perfect for E'_0, and thus affects the γ's as well. We decided to "cure" these deficiencies by using matrix elements calculated from experimental Luttinger parameters (Table III) and experimental E'_0's (Table II). These values are presented in the third row of Table IV.

Since we use parameters which we derive from our LMTO calculations in order to obtain the γ's with perturbation theory, one might argue that this method can be described as a puppy chasing its tail. This is, to some degree, true, but our procedure yields two additional pieces of information: (1) We obtain the sign of the γ's in a simple, natural way. This turns out to be very helpful for the determination of the signs of C_k and C'_k, the coefficients of the linear terms in k (see below). (2) If the LMTO and $\mathbf{k}\cdot\mathbf{p}$ (perturbation theory) values agree within reasonable limits, then we know that the approximations made (pure J_z eigenstates, the value of Δ^- and P', convergence of fourth-order perturbation theory, the number of terms included) are valid. An experimentalist will, of course, measure the "experimentally adjusted" values.

B. Terms linear in k

The existence of spin splittings linear in k in zinc-blende-type materials around the Γ_8 valence bands has been known for a long time.[13,14] They have been measured using magneto-optical[47] and polariton-scattering experiments[48,49] and result in a slight shift of the position of the top of the heavy- $(\frac{3}{2},\pm\frac{3}{2})$ and light-hole $(\frac{3}{2},\pm\frac{1}{2})$ Γ^v_8 bands for $\mathbf{k}$ along the $\langle 110\rangle$ directions. Whereas these splittings do not occur along the $\langle 100\rangle$ directions, they split the $(\frac{3}{2},\pm\frac{3}{2})$ Γ^v_8 and $(\frac{3}{2},\pm\frac{3}{2})$ Γ^c_8 bands for $\mathbf{k}$ along the $\langle 111\rangle$ ones. We designate the corresponding coefficients C_k and C'_k, respectively.

It has been demonstrated[17] that the main contribution to C_k is the second-order interaction, bilinear in $\mathbf{k}\cdot\mathbf{p}$ and in the spin-orbit operator $H_{\rm s.o.}$, between the Γ^v_8 states and the uppermost d core levels (Γ_{12} intermediate states), and that the contribution of the k-dependent spin-orbit Hamiltonian, which follows from first-order perturbation theory, can be neglected.[18]

We present in Fig. 8 the splittings of the $(\frac{3}{2},\pm\frac{3}{2})$ valence (hh) and conduction bands (he) for $\mathbf{k}$ along the [111] direction. The symmetries are Λ_5 and Λ_4. For small k, the splitting is linear, and is related to the C_k's via[13,14]

$$E(\Lambda_5)-E(\Lambda_4)=2\sqrt{2}C_k k\ . \quad (5.5)$$

We have determined the values by fitting the slope for small k and listed them in Table IV. The signs were determined from Figs. 9 and 10, i.e., from the superposition of the linear and cubic splitting terms along the [110] direction.

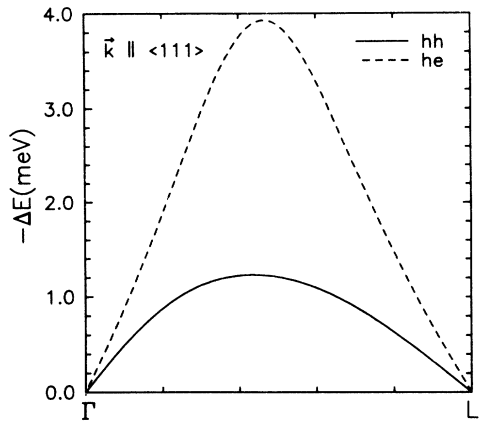

FIG. 8. Spin splittings of the heavy-hole (hh) and heavy-electron (he) $\Gamma_8^{v,c}$ bands in GeSi for **k** along Λ as calculated with the LMTO method.

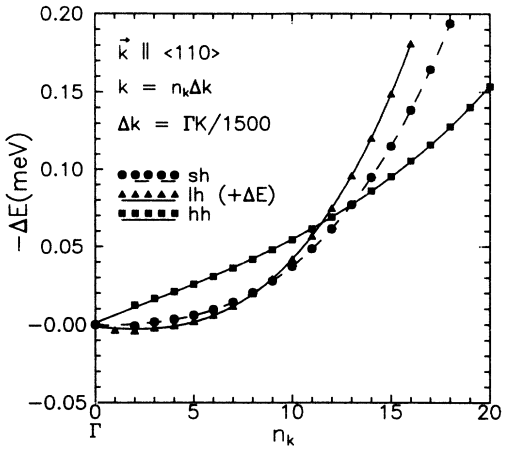

FIG. 10. Detail of the spin splitting of the highest valence bands very close to point Γ in GeSi. Compare this plot with Fig. 7, which shows the splitting along the whole Σ line.

Figures 6 and 7 show the splittings of the lowest conduction and the highest valence bands along Σ. They are rather big, compared with the splittings along [111] since cubic and higher-order terms also contribute. The cubic terms can still be detected in these figures, but not the linear ones. For this reason we show expanded plots of the se, he, le, and *c* bands in Fig. 9, and of the sh, lh, and hh bands in Fig. 10. The k linear terms of the he, le, hh, and lh can be seen in these figures, although they are extremely small compared to values for III-V compounds.[18] Except for the le and lh bands, which have positive γ's, $-\Delta E$ is plotted in these figures. From the plot (Fig. 9), we conclude that C_k' has to have the opposite sign of $\gamma_{\rm le}$, i.e., $C_k'<0$, but the same as $\gamma_{\rm he}$ [see Eq. (5.6)]. From Fig. 10, C_k is seen to have the opposite sign of $\gamma_{\rm lh}$, and C_k is therefore negative.

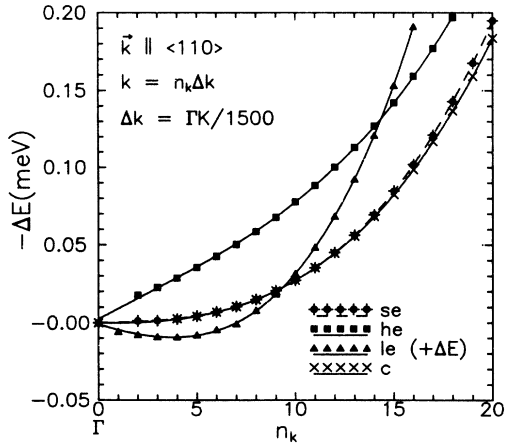

FIG. 9. Detail of the spin splitting of the lowest conduction bands along Σ very close to point Γ in GeSi. The lines represent third-order polynomial fits of the calculated points. The terms linear and cubic in k can easily be discerned, and their signs determined.

As a consequence of the nearly isotropic nature of the valence bands, the linear splitting of the lh to the hh band for **k** along the [110] direction should be in the 1:3 ratio. This follows from the calculations in the region of a quadratic (effective-mass) splitting larger than the linear one[13,14] under the assumption, that the lh and hh eigenstates still have symmetries $(\frac{3}{2},\pm\frac{1}{2})$ and $(\frac{3}{2},\pm\frac{3}{2})$ [note that both splittings have the same sign, as described in Eq. (1) of Ref. 17]:

$$E_{\rm hh}(\Sigma_4)-E_{\rm hh}(\Sigma_3)=\frac{3\sqrt{3}}{2}C_k k\ ,$$
$$E_{\rm lh}(\Sigma_4)-E_{\rm lh}(\Sigma_3)=\frac{\sqrt{3}}{2}C_k k\ . \tag{5.6}$$

Fitting the two splittings to an expression which contains linear and cubic terms, we find a ratio of 3.4 for the linear splittings of the Γ_8^v bands, but only 1.8 for the Γ_8^c bands. This fact reflects again the nonspherical nature of the conduction bands, and asserts, within roundoff errors, that j and m_j are still good quantum numbers for the Γ_v^8 states along the [110] direction.

From the splittings shown in Fig. 10, we obtain $C_k=-1.80$ meV Å, which is almost the same value we calculated for the ⟨111⟩ directions (-1.85 meV Å).

As mentioned earlier, C_k is mainly due to bilinear second-order perturbation terms, including $H_{\mathbf{k}\cdot\mathbf{p}}$ and $H_{\rm s.o.}$, with the Γ_{12} (core *d* states) as intermediate states. Since there are no *d* states in Si, we only take one term of the interpolation formula suggested in Ref. 17:

$$C_k=-A\frac{\Delta_d^{\rm Ge}}{E(\Gamma_8^v)-E_d^{\rm Ge}}\ , \tag{5.7}$$

where $\Delta_d^{\rm Ge}$ is the spin-orbit splitting of the Ge $3d$ level and $E_d^{\rm Ge}$ the energy. Taking values from Ref. 50 and $A=220$ meV Å, as suggested for group-IV materials,[17,18]

we find $C_k = -4.0$ meV Å, which is off by more than a factor of 2 compared to our LMTO values. For III-V compounds the agreement is usually much better.[17,18] As this is the first group-IV compound that has ever been calculated with this value for A, one might be tempted to state that A (which was taken from the average of a cation and anion parameter) for group-IV materials should be smaller than extrapolated from III-V and II-VI values. On the other hand, the fact that Si does not have occupied d states might have unexpected effects on the splitting which cannot be described accurately by Eq. (5.7). We should also keep in mind that the inversion asymmetry of GeSi is mainly of spin-orbit origin, contrary to the case of III-V and II-VI compounds where it is of orbital nature.

A negative value for C_k' is unusual but consistent[18] with the case of InP, which also lacks core d levels in the anion. Any more quantitative agreement between the C_k' of GeSi and those of other zinc-blende-type materials could not be found. This supports the explanation that small C_k''s are due to yet unidentified contributions of other states than the d levels of the cation. It should be mentioned, however, that the sum of C_k and C_k' amounts to the value obtained from Eq. (5.7).

VI. IONICITY AND TRANSVERSE EFFECTIVE CHARGE OF GeSi

The concept of ionicity is somewhat qualitative: elemental tetrahedral semiconductors have zero ionicity while the ionicity increases for the III-V, II-VI, and I-VII compounds. Several attempts have been made to quantify this concept. The ionicity can, of course, be related to the difference in electronegativities C (another qualitative concept) of the constituents.[51,52] For the zinc-blende compounds GeSi, Van Vechten[53,54] calculated $C=0.25$, with Ge acting as the cation. Another ionicity scale[43] is related to the dielectric constant of the materials: increasing ionicity decreases this dielectric constant (which is mainly of covalent origin).[52,54] This "Phillips–Van Vechten" ionicity can be related to the energies of sp^3 hybrids and their hopping or overlap integral. Harrison[42] has defined a polarity α_p, roughly related to the square root of the ionicity, from tight-binding parameters of the p-valence orbitals [see Eq. (3.7)],

$$\alpha_p = \frac{E_p^c - E_p^a}{[(E_p^c - E_p^a)^2 + H_{xx}^2]^{1/2}} , \tag{6.1}$$

where E_p^c and E_p^a are the term energies of cation and anion, respectively.

An empirical ionicity was defined by the Kowalczyck *et al.*[55] based on the splitting of the two s-like peaks seen in the x-ray photoemission spectroscopy (XPS) spectra of the valence bands. From the splittings of the two lowest valence bands at the L points, shown in Figs. 2–4, we estimate this ionicity to be, for GeSi, 0.07 (*with Ge more electronegative than Si*), a rather small value. The same value has been obtained in Ref. 43 for Harrison's polarity α_p (*but this time with Si more electronegative than Ge*), while a value $f_i = 0.00$ was found for the Phillips–Van Vechten ionicity. All these estimates indicate that the ionicity (polarity) of GeSi should be very small, so that even its sign is questionable, in contrast to the only group-IV zinc-blende-type material which exists in nature, SiC, for which the ionicity is ≈ 0.4,[43] as corresponds to the large electronegativity of C compared with that of Si.

GeSi is, like other zinc-blende-structure compounds, an infrared-active material: the optical phonon at point Γ is associated with an electric dipole moment which can be represented by the transverse effective charge e_T^*. It is of interest to estimate e_T^*; when considered as a band effective charge, e_T^* may also help to estimate the infrared activity of phonons in Ge/Si superlattices. In terms of α_p and its volume derivative, e_T^* is given by [see Eq. (49) of Ref. 43]

$$e_T^* = 4\left[\alpha_p + \frac{d\alpha_p}{d\ln V}\right] . \tag{6.2}$$

Using the values of α_p and $d\alpha_p/d\ln V$ given in Table VI of Ref. 43 for GeSi, we find $e_T^* = 4(0.07 - 0.047) = +0.09$, the + sign implying that the negative charge resides on the Si (again Ge plays the role of the cation). This value of e_T^* is very small compared with that found by typical III-V or II-VI compounds (around 2.3) and also for SiC (2.7).[43,56] Hence the phonon-induced infrared absorption, proportional to $|e_T^*|^2$, should be negligible for GeSi and Ge/Si superlattices.

We should remark that e_T^* can also be estimated from empirical pseudopotential parameters.[57] Using this method, we obtain $e_T^* = -0.6 \pm 0.3$, but now with the negative charge located on the Ge. As pointed out in Sec. III B, however, we have good reasons to believe that only self-consistent calculations yield the right charge transfer that occurs in GeSi, so that this conflict in sign is not surprising. Therefore we can say with certainty that e_T^* is small, with probably a positive sign.

VII. CONCLUSIONS

We have calculated the band structures of Si, Ge, and zinc-blende-type GeSi using the LMTO method with an "*ad hoc*" correction of the LDA "gap problem." From these band structures, effective masses and Luttinger parameters of states around the gap at $\mathbf{k}=\mathbf{0}$ (Γ point) have been numerically obtained. The rest of the paper has been devoted to the investigation of inversion-asymmetry effects in the LMTO band structure of GeSi and to describe them in terms of parametrized $\mathbf{k}\cdot\mathbf{p}$ and tight-binding perturbation theories. Such effects include the Δ^- spin-orbit coupling of the Γ_{15} valence and conduction bands, the spin splittings cubic and linear in k, and, last but not least, the ionicity (polarity) and the infrared effective charge e_T^*. It has been shown that orbital-inversion-asymmetry effects are small, and that we cannot even say with absolute certainty whether Si is more or less electronegative than Ge. Correspondingly, $e_T^* \approx 0.1$, as obtained with the tight-binding approach (or even the somewhat larger $|e_T^*| = 0.6$ obtained with pseudopotentials) should lead to insignificant infrared absorp-

tion for sample thicknesses compatible with MBE-growth techniques (a few μm). The main difference in the band structures of Si and Ge is the low $\Gamma_{2'}$ conduction band, known to be due to relativistic mass-velocity effects g. The remaining orbital-band states are nearly the same for Ge and Si, a factor which results in a rather small inversion asymmetry: the region around $\Gamma_{2'}$ has nearly zero weight in $\mathbf{k}$ space.

We have thus demonstrated that the main contribution to the inversion asymmetry of GeSi originates in the spin-orbit interaction: the spin-orbit splittings of the $\Gamma_{25'}$ states of Ge (0.3 eV) and Si (0.04 eV) are very different and Ge has spin-orbit-split $3d$ core levels which are absent in Si. These splittings result in a Δ^- coupling between Γ_{15}^c and Γ_{15}^v in GeSi, plus spin splittings at a given $\mathbf{k}$ in all directions except the [100]. These splittings have been evaluated and interpreted in terms of parametrized $\mathbf{k}\cdot\mathbf{p}$ theory. Around $\mathbf{k}=0$ they are odd in k, the first relevant power being k^3 for the lowest conduction band and the spin-orbit-split Γ_7 bands. For the Γ_8 bands, however, linear terms, related to spin-orbit splittings of core levels, arise. Experimental determination of these coefficients should be possible with improvement in MBE preparation techniques. We point out that the k^3 terms should give rise to splittings linear in k in superlattices $(\mathrm{Ge})_n/(\mathrm{Si})_m$, provided that both n and m are odd.[58] We are planning to use the techniques developed here to investigate the band structure of these superlattices.

ACKNOWLEDGMENTS

We thank S. G. Louie and M. P. Surh for fruitful discussions, and for pointing out to us an error in the determination of the sign of C_k of the hh band.

[1]T. P. Pearsall, J. Bevk, L. C. Feldman, J. M. Bonar, J. P. Mannaerts, and A. Ourmazd, Phys. Rev. Lett. **58**, 729 (1987).
[2]M. S. Hybertsen, M. Schlüter, R. People, S. A. Jackson, D. V. Lang, T. P. Pearsall, J. C. Bean, J. M. Vandenberg, and J. Bevk. Phys. Rev. B **37**, 10 195 (1988).
[3]E. Kasper, H. Kibbel H. Jorke, H. Brugger, E. Friess, and G. Abstreiter, Phys. Rev. B **38**, 3599 (1988).
[4]T. P. Pearsall, J. Bevk, J. C. Bean, J. Bonar, J. P. Mannaerts, and A. Ourmazd, Phys. Rev. B **39**, 3741 (1989), and references therein.
[5]M. I. Alonso, M. Cardona, and G. Kanellis, Solid State Commun. **69**, 479 (1989); Solid State Commun. **70**, i (1989).
[6]S. Satpathy, R. M. Martin, and C. G. Van de Walle, Phys. Rev. B **38**, 13 237 (1988).
[7]S. Froyen, S. M. Wood, and A. Zunger, Phys. Rev. B **36**, 1310 (1987).
[8]S. Ciraci and I. P. Batra, Phys. Rev. Lett. **58**, 2114 (1987).
[9]S. Ciraci and I. P. Batra, Phys. Rev. B **38**, 1835 (1988).
[10]M. S. Hybertsen and M. Schlüter, Phys. Rev. B **36**, 9683 (1981).
[11]I. Morrison, M. Jaros, and K. B. Wong, Phys. Rev. B **37**, 9693 (1987).
[12]K. B. Wong, M. Jaros, I. Morrison, and J.P. Hagon, Phys. Rev. Lett. **60**, 2221 (1988).
[13]G. Dresselhaus, Phys. Rev. B **186**, 824 (1958).
[14]E. O. Kane, in *Semiconductors and Semimetals,* edited by R. K. Willardson and A. C. Beer (Academic, New York, 1966), Vol. 1, pp. 75 and 94.
[15]M. Cardona, F. H. Pollak, and J. G. Broerman, Phys. Lett. **19**, 276 (1965).
[16]N. E. Christensen and M. Cardona, Solid State Commun. **51**, 491 (1984).
[17]M. Cardona, N. E. Christensen, and G. Fasol, Phys. Rev. Lett. **56**, 2831 (1986).
[18]M. Cardona, N. E. Christensen, and G. Fasol, Phys. Rev. B **38**, 1806 (1988) (note that all inversion-asymmetry splittings of the lh and le bands are given with the wrong sign in this paper; the corresponding γ's thus have the wrong sign).
[19]N. E. Christensen, I. Gorczyca, O. B. Christensen, U. Schmid, and M. Cardona, J. Cryst. Growth (to be published).
[20]M. I. Diakonov and V. I. Perel, in *Optical Orientation,* edited by V. M. Agranovich and A. A. Maradudin (North-Holland, Amsterdam, 1984), p. 11.
[21]A. T. Gorelenko, B. A. Marushchak, and A. N. Titkov, Izv. Akad. Nauk SSSR, Ser. Fiz. **50**, 290 (1986).
[22]W. Kauschke, N. Mestres, and M. Cardona, Phys. Rev. B **35**, 3843 (1987).
[23]H. Riechert, S. F. Alvarado, A. N. Titkov, and V. I. Safarov, Phys. Rev. Lett. **52**, 2297 (1984).
[24]Y. Nozue, M. Itoh, and K. Cho, J. Phys. Soc. Jpn. **50**, 889 (1981).
[25]Y. F. Chen, M. Dobrowolska, J. K. Furdyna, and S. Rodriguez, Phys. Rev. B **32**, 890 (1985).
[26]M. Cardona, N. E. Christensen, M. Dobrowolska, J. K. Furdyna, and S. Rodriguez, Solid State Commun. **60**, 171 (1986).
[27]O. K. Andersen, Phys. Rev. B **12**, 3060 (1975).
[28]D. Glötzel, B. Segal, and O. K. Andersen, Solid State Commun. **36**, 403 (1980).
[29]J. M. Luttinger, Phys. Rev. **102**, 1030 (1955).
[30]M. Cardona, J. Phys. Chem. Solids **24**, 1543 (1963).
[31]P. Lawaetz, Phys. Rev. B **4**, 3460 (1971).
[32]*Landolt-Börnstein Tables,* edited by O. Madelung, M. Schulz, and H. Weiss (Springer, Berlin, 1982), Vol. 17a, and references therein.
[33]U. Rössler, Solid State Commun. **49**, 943 (1984).
[34]P. Hohenberg and W. Kohn, Phys. Rev. **136**, B964 (1964); W. Kohn and L. J. Sham, *ibid.* **140**, A1133 (1965).
[35]G. B. Bachelet and N. E. Christensen, Phys. Rev. B **31**, 879 (1985).
[36]D. M. Ceperley and B. J. Adler, Phys. Rev. Lett. **45**, 566 (1980).
[37]J. Perdew and A. Zunger, Phys. Rev. B **23**, 5048 (1981).
[38]N. E. Christensen, Phys. Rev. B **30**, 5753 (1984).
[39]J. A. Van Vechten, Phys. Rev. **187**, 1007 (1969).
[40]R. L. Bowers and G. D. Mahan, Phys. Rev. **185**, 1973 (1969).
[41]A. Blacha, H. Presting, and M. Cardona, Phys. Status Solidi B **126**, 11 (1984).
[42]W. A. Harrison, *Electronic Structure and the Properties of Solids* (Freeman, San Francisco, 1980). In Eq. (3.8) we actually use the parameters of the sp^3s^* model, W. A. Harrison, Phys. Rev. B **24**, 5835 (1981).
[43]N. E. Christensen, S. Satpathy, and Z. Pawlowska, Phys. Rev. B **36**, 1032 (1987).
[44]M. L. Cohen and T. K. Bergstresser, Phys. Rev. **141**, 789 (1966).
[45]M. Cardona, *Modulation Spectroscopy* (Academic, New York,

1969).
[46]M. Cardona and F. H. Pollak, Phys. Rev. **142**, 530 (1966).
[47]C. R. Pidgeon and S. H. Groves, Phys. Rev. **186**, 824 (1969).
[48]B. Höhnerlage, U. Rössler, V. D. Phach, A. Bivas, and J. B. Grun, Phys. Rev. B **22**, 797 (1980).
[49]R. Sooryakumar, M. Cardona, and J. C. Merle Phys. Rev. B **30**, 3261 (1984).
[50]L. Ley and M. Cardona, in *Photoemission in Solids II,* edited by L. Ley and M. Cardona (Springer, Heidelberg, 1979), p. 377.
[51]L. Pauling, *The Nature of the Chemical Bond* (Cornell University Press, Ithaca, NY, 1960).
[52]J. C. Phillips, *Bonds and Bands in Semiconductors* (Academic, New York, 1973).
[53]J. A. Van Vechten and T. K. Bergstresser, Phys. Rev. B **1**, 3351 (1970).
[54]J. A. Van Vechten, Phys. Rev. **182**, 891 (1969).
[55]S. Kowalczyck, L. Ley, F. R. McFeely, and D. A. Shirley, J. Chem. Phys. **61**, 2850 (1974).
[56]E. Anastassakis and M. Cardona, Phys. Status Solidi B **129**, 101 (1985).
[57]R. Trommer, H. Müller, M. Cardona, and P. Vogl, Phys. Rev. B **21**, 4869 (1980).
[58]S. Gopalan, M. Cardona, and N. E. Christensen, Solid State Commun. **66**, 471 (1988).